

Dressed Bose-Einstein Condensates in High-Q Cavities

Elena V. Goldstein, Ewan M. Wright and P. Meystre

Optical Sciences Center, University of Arizona, Tucson, AZ 85721

Abstract

We propose and analyze a way in which effective multicomponent condensates can be created inside high-Q multimode cavities. In contrast to the situation involving several atomic species or levels, the coupling between the various components of the dressed condensates is linear. We predict analytically and numerically confirm the onset of instabilities in the quasiparticle excitation spectrum.

PACS numbers: 03.75.Fi

arXiv:cond-mat/9710322v2 31 Oct 1997

I. INTRODUCTION

The Bose-Einstein condensation of low density atomic samples [1,2] provides one with a new paradigm in many-body theory, atomic physics, quantum optics, and nonlinear dynamics. Below the critical temperature, condensates are described to an excellent degree of accuracy by a scalar nonlinear Schrödinger equation, the Gross-Pitaevskii equation describing the dynamics of the condensate wave function [3–6]. The elementary excitations of the condensate evaluated from a Bogoliubov linearization about the condensate solution are in good qualitative agreement with experiments [7–14], and so is the Hartree mean-field energy of the system [15,16].

Nonlinear Schrödinger equations are of course ubiquitous in physics, and have been studied in great detail in the past, in situations from fluid dynamics [17] to phenomenological models of field theories [18] and to nonlinear optics [19]. They play an important role in the study of pattern formation in beam propagation [20], and their soliton solutions find applications in problems such as light propagation in fibers [21]. From this work, it is known that the dynamical and stability properties of multicomponent nonlinear Schrödinger equations can be vastly different from those of their scalar versions, and lead to a wealth of new effects [21–24]. It would be of considerable interest to generalize these ideas to the case of matter waves and to have multicomponent condensates available.

While it is not generally possible to create two coexisting condensates inside a trap, exceptions are possible, as recently demonstrated in Rubidium experiments by the JILA group [25]. However, this coexistence relies on a fortuitous coincidence of the scattering lengths for the two Zeeman sublevels involved [26], a coincidence that cannot be generally counted on. There are proposals to optically change the s-wave scattering length of ground state atoms [27], but whether this can be used to produce coexisting condensates remains to be seen. The goal of the present paper is to propose and analyze a method by which effective multicomponent condensates can be generated inside a high-Q multimode optical resonator. The cavity photons dress the condensate, very much like atoms can be dressed

by electromagnetic fields [28], and the various dressed condensate states are coupled, e.g. via an electric dipole interaction. Hence, the condensate inside the cavity should be thought of as a coupled multicomponent system, each component subject to a nonlinear equation, and in addition coupled to its neighboring components. In contrast to the situation involving two (or more) atomic species or levels, the coupling between the various components of the dressed condensate is linear, rather than resulting from collisions and hence nonlinear. Nonetheless, we submit that this method permits to generate and study "coupled condensates" in a controllable — and at least in principle simple — way.

This paper is organized as follows: Section II defines our model and uses a Hartree variational principle to derive coupled nonlinear Schrödinger equations describing the evolution of a dressed condensate in a two-mode cavity. Section III specializes to the case where only one photon is present inside the resonator, and thus only two dressed condensate components are of importance. In that case, the problem reduces to the so-called discrete self-trapping equations for a dimer familiar in nonlinear physics. These equations are integrable in free space, but not in the trap situation that we consider here. We solve them approximately in the Thomas-Fermi approximation and study the spectrum of elementary excitations. We predict the onset of instabilities in the system, and compare these analytical results with an exact numerical solution of the equations. Finally, Section IV is a summary and conclusion.

II. PHYSICAL MODEL

A. Basic theory

Our model system comprises a Bose-Einstein condensate (BEC) which interacts with two counter-propagating modes supported by a high-Q ring cavity. We assume a cavity QED configuration [29] and neglect all field modes except the two of interest, so that the electric field operator can be written as

$$\mathbf{E}(\mathbf{r}, t) = i\hat{\epsilon}\mathcal{E}_p \left[a_1 e^{ikz} + a_2 e^{-ikz} \right] e^{-i\omega_c t} + h.c., \quad (1)$$

where $\hat{\mathbf{e}}$ is the unit polarization vector of the light, $\mathcal{E}_p = \sqrt{\hbar\omega_c/2\epsilon_0 V}$ is the electric field per photon for light of frequency ω_c in a mode volume V , $k = \omega_c/c = 2\pi/\lambda_c$ the light wavevector, and $a_{1,2}$, and $a_{1,2}^\dagger$ are annihilation and creation operators of the cavity modes satisfying Bose commutation relations $[a_i, a_j^\dagger] = \delta_{ij}$. For this treatment we neglect the detailed mode structure of the field in the transverse plane perpendicular to the optical-axis z , assuming that it is homogeneous on the spatial scale of the BEC, and that it is unaffected by its presence.

The atoms comprising the condensate are confined by an external trapping potential $U(\mathbf{r})$ which binds the atoms on a sub-wavelength scale along the longitudinal axis z . In addition they interact with the cavity field, which induces transitions between the ground and excited electronic states. The single-particle Hamiltonian H_0 for the atoms, in an interaction picture with the optical frequency removed, then reads [30]

$$H_0 = \frac{\mathbf{p}^2}{2m} + U(\mathbf{r}) + \hbar\delta\sigma_+\sigma_- + \hbar\Omega_0[\sigma_+(a_1 + a_2) + \sigma_-(a_1^\dagger + a_2^\dagger)], \quad (2)$$

where we have located the BEC at $z = 0$ without loss of generality, \mathbf{p} is the center-of-mass atomic momentum, m the atomic mass, $\delta \equiv \omega_a - \omega_c$ is atom-field detuning, ω_a being the atomic transition frequency, $\Omega_0 = d\mathcal{E}_p/\hbar$ is the strength of the atom-field coupling, d being the atomic dipole-matrix element, and σ_+ , σ_- are pseudo-spin atomic raising and lowering operators for transitions between the ground and excited atomic states. We consider the case of large atom-field detuning for which the excited atomic state can be adiabatically eliminated. This results in the following effective single-particle Hamiltonian (see Appendix A for details) involving only the ground atomic state

$$H_{eff} = \frac{\mathbf{p}^2}{2m} + U(\mathbf{r}) + \frac{\hbar\Omega_0^2}{\delta} (a_1^\dagger a_1 + a_2^\dagger a_2 + a_2^\dagger a_1 + a_1^\dagger a_2). \quad (3)$$

The four terms involving field mode operators in this effective Hamiltonian describe virtual transitions involving the absorption of a photon from mode 1 followed by re-emission into mode 1, the same but for mode 2, absorption of a photon from mode 1 followed by re-emission into mode 2, and vice versa. The last two of these processes are allowed since the length δz

of the BEC is taken to be less than an optical wavelength, yielding an associated momentum uncertainty $\delta p_z \approx \hbar/\delta z > 2\hbar k$. Hence the momentum deficit involved in the transfer of a photon from one direction to the other around the cavity is within the Heisenberg uncertainty principle. We also note that the effective Hamiltonian conserves the total number of photons $n = (a_1^\dagger a_1 + a_2^\dagger a_2)$ which is then a good quantum number.

Proceeding now to include many-body interactions, the second-quantized Hamiltonian describing our system is [3]

$$\mathcal{H} = \int d1d2 \langle 1|H_{eff}|2\rangle \Psi^\dagger(1)\Psi(2) + \frac{1}{2} \int d\{\ell\} \langle 1, 2|V|3, 4\rangle \Psi^\dagger(1)\Psi^\dagger(2)\Psi(3)\Psi(4), \quad (4)$$

where ℓ denotes a full set of quantum numbers, and $\Psi(\ell)$ and $\Psi^\dagger(\ell)$ are the usual atomic field annihilation and creation operators, which for bosonic atoms satisfy the commutation relations

$$[\Psi(\ell), \Psi^\dagger(\ell')] = \delta(\ell - \ell'). \quad (5)$$

The two-body potential is in the limit of s-wave scattering [3]

$$V(\mathbf{r}_1, \mathbf{r}_2) = \hbar V_0 \delta(\mathbf{r}_1 - \mathbf{r}_2), \quad (6)$$

where $V_0 = 4\pi\hbar a/m$ measures the strength of the two-body interaction, a being the s-wave scattering length. Here we consider a repulsive interaction so that $a > 0, V_0 > 0$.

B. Coupled-condensate equations

The second-quantized Hamiltonian for our system conserves both the number of atoms and the total number of photons, so we consider a state comprising N atoms and n photons. The state of the system can be written in the form

$$|\Psi_{N,n}(t)\rangle = \sum_{n_1+n_2=n} \int d\mathbf{r}_1 \dots \int d\mathbf{r}_N f_{n_1,n_2}(\mathbf{r}_1, \dots, \mathbf{r}_N, t) \Psi^\dagger(\mathbf{r}_1) \dots \Psi^\dagger(\mathbf{r}_N) |0, n_1, n_2\rangle, \quad (7)$$

where the summation runs over all positive integers $n_{1,2}$ obeying $n_1 + n_2 = n$, $f_{n_1,n_2}(\mathbf{r}_1, \dots, \mathbf{r}_N, t)$ is the many-particle Schrödinger wave function for the BEC given there

are n_1 photons in mode 1 and n_2 photons in mode 2, and $|0, n_1, n_2\rangle$ is the state with no ground state atoms present, n_1 photons in mode 1 and n_2 photons in mode 2. To proceed we invoke the Hartree approximation, which is appropriate for a Bose condensed system in which the atoms are predominantly in the same state. The Hartree approximation is therefore strictly valid at zero temperature, and for a weakly interacting Bose gas as assumed here, so that the condensate fraction is close to unity [3]. Accordingly the many-particle wave function is written as a product of Hartree wave functions

$$f_{n_1, n_2}(\mathbf{r}_1, \dots, \mathbf{r}_N, t) = \prod_{i=1}^N \phi_{n_1, n_2}(\mathbf{r}_i, t). \quad (8)$$

Here $\phi_{n_1, n_2}(\mathbf{r}, t)$ is the Hartree wave function which represents the state the atoms occupy. The equation of motion for $\phi_{n_1, n_2}(\mathbf{r}, t)$ results from the Hartree variational principle [31]

$$\frac{\delta}{\delta \phi_{n_1, n_2}^*} \left[\langle \Psi_{N, n}(t) | i\hbar \frac{\partial}{\partial t} - \mathcal{H} | \Psi_{N, n}(t) \rangle \right] = 0, \quad (9)$$

and takes the form of a system of coupled nonlinear Schrödinger equations, or Gross-Pitaevskii equations

$$i\hbar \dot{\phi}_{n_1, n_2}(\mathbf{r}, t) = \left[-\frac{\hbar^2}{2m} \nabla^2 + U(\mathbf{r}) \right] \phi_{n_1, n_2}(\mathbf{r}, t) + \hbar V_0 N |\phi_{n_1, n_2}(\mathbf{r}, t)|^2 \phi_{n_1, n_2}(\mathbf{r}, t) \\ + \frac{\hbar \Omega_0^2}{\delta} \left(\sqrt{n_1(n_2 + 1)} \phi_{n_1 - 1, n_2 + 1}(\mathbf{r}, t) + \sqrt{(n_1 + 1)n_2} \phi_{n_1 + 1, n_2 - 1}(\mathbf{r}, t) \right), \quad (10)$$

where the photon numbers $n_{1,2}$ in modes 1 and 2 again run over all positive integers obeying $n_1 + n_2 = n$. In the limit $\Omega_0 = 0$ there is no coupling between the cavity modes and the BEC and Eq. (10) is the usual scalar Gross-Pitaevskii equation for the condensate. In contrast, for non-zero values of Ω_0 the processes involving absorption of a photon from one direction and re-emission into the other direction lead to a linear coupling between the state with (n_1, n_2) photons and those with $(n_1 - 1, n_2 + 1)$ and $(n_1 + 1, n_2 - 1)$ photons, the notation (n_1, n_2) meaning n_1 photons in state 1 and n_2 photons in state 2. As a result, the system is generally a superposition of states with different (n_1, n_2) .

As they stand, Eqs. (10) account for the full three-dimensional structure of the BEC. In order to make our presentation as straightforward as possible we now make some further

simplifying assumptions, but we stress that these are not essential and do not limit the generality of the conclusions that we draw. To proceed we write the trapping potential explicitly as [4–6]

$$U(\mathbf{r}) = \frac{m\omega_{\perp}^2}{2} (\mathbf{r}_{\perp}^2 + \lambda^2 z^2), \quad (11)$$

thereby separating the longitudinal potential out from the transverse trapping potential. Here $\mathbf{r} = (\mathbf{r}_{\perp}, z)$, \mathbf{r}_{\perp} being the transverse position coordinate, ω_{\perp} the transverse angular frequency of the trap, and $\lambda = \omega_z/\omega_{\perp}$ is the ratio of the longitudinal to transverse frequencies. Here we assume that $\lambda \ll 1$ so that the longitudinal trapping is much weaker than the transverse trapping, hence giving the BEC density profile a cigar structure [16].¹ Specifically, we assume that the transverse structure of the BEC is not significantly altered by many-body interactions and is determined as the ground state solution of the transverse potential

$$\hbar\omega_{\perp}v_g(\mathbf{r}_{\perp}) = \left[-\frac{\hbar^2}{2m}\nabla_{\perp}^2 + \frac{m\omega_{\perp}^2}{2}\mathbf{r}_{\perp}^2 \right] v_g(\mathbf{r}_{\perp}), \quad (12)$$

and we express the Hartree wave function as

$$\phi_{n_1, n_2}(\mathbf{r}, t) = v_g(\mathbf{r}_{\perp}) e^{-i\omega_{\perp}t} \phi'_{n_1, n_2}(z, t). \quad (13)$$

Substituting this expression into Eq. (10), projecting out the transverse mode, and dropping the prime for simplicity in notation, yields the coupled Gross-Pitaevskii equations for the quasi-one-dimensional system. Introducing the dimensionless length $\xi = z/a_z$, $a_z \equiv \sqrt{\hbar/2m\omega_z}$ being the characteristic length associated with the longitudinal trapping potential, and the dimensionless time $\tau = \omega_z t$, these coupled equations can be written in the scaled form

¹The opposite case of weak transverse trapping $\lambda \gg 1$ corresponds to the BEC having a pancake structure [1] and alters only the dimensionality of the resulting equations. In particular it leads to a two-dimensional rather than a one-dimensional problem.

$$\begin{aligned}
i\dot{\phi}_{n_1, n_2}(\xi, \tau) &= H_L \phi_{n_1, n_2}(\xi, \tau) + \eta |\phi_{n_1, n_2}(\xi, \tau)|^2 \phi_{n_1, n_2}(\xi, \tau) \\
&+ g \left(\sqrt{n_1(n_2 + 1)} \phi_{n_1-1, n_2+1} + \sqrt{(n_1 + 1)n_2} \phi_{n_1+1, n_2-1} \right),
\end{aligned} \tag{14}$$

where the Hamiltonian H_L is given by

$$H_L = \left[-\frac{\partial^2}{\partial \xi^2} + \frac{1}{4} \xi^2 \right], \tag{15}$$

$g = \Omega_0^2 / \delta\omega_z$ is the atom-field interaction energy per photon in units of $\hbar\omega_z$, which acts as the coupling coefficient between different states (n_1, n_2) , and

$$\eta = \frac{NV_0/\mathcal{V}}{\omega_z} = \frac{NV_0}{a_z\omega_z} \frac{\int d\mathbf{r}_\perp |v_g(\mathbf{r}_\perp)|^4}{\int d\mathbf{r}_\perp |v_g(\mathbf{r}_\perp)|^2}, \tag{16}$$

is the many-body interaction energy for N atoms in a volume \mathcal{V} in units of $\hbar\omega_z$.

Equations (14) are the basis of the remainder of this paper. The transformation to dimensionless variables reveals that the key parameters for the system are the linear coupling coefficient g , and the nonlinear parameter η describing self-phase modulation.

III. DRESSED BOSE-EINSTEIN CONDENSATES

A. Dressed BECs

The dressed BECs are the eigenstates of Eqs. (14) (or more generally Eqs. (10)), and are quantum superpositions of states with different photon numbers (n_1, n_2) . Setting

$$\phi_{n_1, n_2}(\xi, \tau) = e^{-i\mu\tau} \theta_{n_1, n_2}(\xi), \tag{17}$$

for the dressed states, we obtain

$$\begin{aligned}
\mu\theta_{n_1, n_2}(\xi) &= H_L \theta_{n_1, n_2} + \eta |\theta_{n_1, n_2}(\xi)|^2 \theta_{n_1, n_2}(\xi) \\
&+ g \left(\sqrt{n_1(n_2 + 1)} \theta_{n_1-1, n_2+1} + \sqrt{(n_1 + 1)n_2} \theta_{n_1+1, n_2-1} \right),
\end{aligned} \tag{18}$$

with μ the chemical potential scaled to $\hbar\omega_z$. Admissible solutions should also be normalized according to

$$\int_{-\infty}^{\infty} d\xi \sum_{n_1+n_2=n} |\theta_{n_1, n_2}(\xi)|^2 = 1. \quad (19)$$

Numerical calculations are generally required to solve these equations for the dressed states, but simple limiting cases can be treated analytically.

B. Single cavity photon, $n = 1$

The essential physics of dressed BECs can be exposed using the simplest case of one cavity photon, $n = 1$, so only the states with $(1, 0)$ and $(0, 1)$ are relevant. Then the coupled time-dependent Eqs. (14) reduce to

$$\begin{aligned} i\dot{\phi}_{01}(\xi, \tau) &= H_L \phi_{01}(\xi, \tau) + g\phi_{10}(\xi, \tau) + \eta|\phi_{01}(\xi, \tau)|^2 \phi_{01}(\xi, \tau), \\ i\dot{\phi}_{10}(\xi, \tau) &= H_L \phi_{10}(\xi, \tau) + g\phi_{01}(\xi, \tau) + \eta|\phi_{10}(\xi, \tau)|^2 \phi_{10}(\xi, \tau), \end{aligned} \quad (20)$$

which yields the following pair of coupled equations for the dressed states

$$\begin{aligned} \mu\theta_{01}(\xi) &= H_L \theta_{01}(\xi) + g\theta_{10}(\xi) + \eta|\theta_{01}(\xi)|^2 \theta_{01}(\xi), \\ \mu\theta_{10}(\xi) &= H_L \theta_{10}(\xi) + g\theta_{01}(\xi) + \eta|\theta_{10}(\xi)|^2 \theta_{10}(\xi). \end{aligned} \quad (21)$$

These systems of equations are similar to those that appear in the theory of multi-component condensates [24]. However, instead of a nonlinear coupling due to cross-phase modulation we have here linear coupling due to the exchange of photons between cavity modes via virtual atomic transitions. In this respect our equations more closely resemble those describing the *linear* evanescent coupling of adjacent nonlinear optical fibers [32].

Equations (20) are known in nonlinear physics as the discrete self-trapping equations for a dimer (see e.g. [22] and references therein). The stationary solutions for such a system were classified and their stability was studied in Ref. [22] in the case $H_L = 0$. Three types of solution for the dimer were uncovered: an in-phase solution denoted $(\uparrow\uparrow)$ for which, in our notation, $\theta_{10} = \theta_{01}$, an out-of-phase solution $(\uparrow\downarrow)$ with $\theta_{10} = -\theta_{01}$, and asymmetric solutions $(\uparrow\cdot)$ and $(\cdot\uparrow)$ with $|\theta_{10}| \neq |\theta_{01}|$.

The same classification scheme can be employed here for the dressed states including the Hamiltonian H_L in Eqs. (21). In this case, however, exact analytic solutions are not available for the dressed states, but approximate solutions can be obtained for the in-phase and out-of-phase solutions within the Thomas-Fermi approximation in which the nonlinear interaction term dominates over the kinetic energy term [6]. In the Thomas-Fermi approximation we then obtain the following dressed state solution from Eqs. (21)

$$\theta_{10}^{\pm}(\xi) = \frac{1}{\eta^{1/2}} \sqrt{\mu \mp g - \frac{1}{4}\xi^2}, \quad (22)$$

when the argument of the square root is greater than or equal to zero, and is zero otherwise. The top sign in Eq. (22) corresponds to the in-phase solution, and the lower one to the out-of-phase solution. The normalization of the wave function then leads to the following expression for the chemical potential of the two solutions

$$\mu^{\pm} = \pm g + \frac{1}{4}\xi_m^2, \quad (23)$$

where $\xi_m = [3\eta/2]^{1/3}$ is the longitudinal coordinate at which the Thomas-Fermi solution vanishes. Using this expression for the chemical potential in Eq. (22) for the dressed state solution we readily find that the profile

$$|\theta_{10}^{\pm}|^2 = \frac{\xi_m^2 - \xi^2}{4\eta} \quad (24)$$

is in fact independent of g and whether it is the in-phase or out-of-phase solution.

C. Elementary excitations

The elementary excitations of the system can be found by linearizing Eqs. (20) around the dressed state solutions

$$\begin{aligned} \phi_{10}(\xi, \tau) &= e^{-i\mu\tau} [\theta_{10}(\xi) + u_{10}(\xi)e^{-i\omega\tau} + v_{10}^*(\xi)e^{i\omega\tau}], \\ \phi_{01}(\xi, \tau) &= e^{-i\mu\tau} [\theta_{01}(\xi) + u_{01}(\xi)e^{-i\omega\tau} + v_{01}^*(\xi)e^{i\omega\tau}], \end{aligned} \quad (25)$$

where $u(\xi)$ and $v(\xi)$ represent small perturbations around the dressed state with energies $\mu \pm \omega$. In zeroth order, substitution of these expressions into Eq. (20) results in the system of two equations (21) for the dressed states. In first-order, it leads to the system of four equations for the linearized perturbations $u(\xi)$ and $v(\xi)$

$$\begin{aligned}
\omega u_{10}(\xi) &= \left[H_L + 2\eta|\theta_{10}(\xi)|^2 - \mu \right] u_{10}(\xi) + g u_{01}(\xi) + \eta \theta_{10}(\xi)^2 v_{10}(\xi), \\
\omega u_{01}(\xi) &= \left[H_L + 2\eta|\theta_{10}(\xi)|^2 - \mu \right] u_{01}(\xi) + g u_{10}(\xi) + \eta \theta_{01}(\xi)^2 v_{01}(\xi), \\
\omega v_{10}(\xi) &= \left[H_L + 2\eta|\theta_{10}(\xi)|^2 - \mu \right] v_{10}(\xi) + g v_{01}(\xi) + \eta \theta_{10}(\xi)^2 u_{10}(\xi), \\
\omega v_{01}(\xi) &= \left[H_L + 2\eta|\theta_{10}(\xi)|^2 - \mu \right] v_{01}(\xi) + g v_{10}(\xi) + \eta \theta_{01}(\xi)^2 u_{01}(\xi).
\end{aligned} \tag{26}$$

The normal modes of this system of coupled equations are identical to the elementary excitations determined via the Bogoliubov method in which the Hamiltonian for the linearized perturbations is brought into diagonal form using a Bogoliubov transformation [33].

It was shown in Ref. [22] that for the case corresponding to $H_L = 0$ the out-of-phase solution ($\uparrow\downarrow$) of the self-trapped equations is always stable, while the in-phase solution ($\uparrow\uparrow$) is stable until it bifurcates at a condition corresponding to $\mu^+ = 2g$, yielding a stable asymmetric branch and an unstable in-phase branch. Here we study the influence of the Hamiltonian H_L on the stability of the in-phase and out-of-phase dressed-states of the system.

An exact solution for the normal modes of Eqs. (26) is not available, to the best of our knowledge. To proceed we therefore use the consequence of the Thomas-Fermi approximation $\xi_m \gg 1$, which means that the profile of the dressed state solution is broad compared to the characteristic length scale of the trapping potential. This allows us to assume $|\theta_{n_1, n_2}^\pm(\xi)|^2 \simeq |\theta_{n_1, n_2}^\pm(\xi = 0)|^2 \approx \xi_m^2/4\eta$ for normal modes localized close to the center of the trapping potential. With this replacement Eqs. (26) can be conveniently solved by expanding the perturbations in terms of eigenfunctions of the linear trapping potential $H_L q_\nu(\xi) = (\nu + 1/2)q_\nu(\xi)$

$$\begin{aligned}
u_{10}(\xi) &= \sum_\nu b_{10}^\nu q_\nu(\xi), & u_{01}(\xi) &= \sum_\nu b_{01}^\nu q_\nu(\xi); \\
v_{10}(\xi) &= \sum_\nu c_{10}^\nu q_\nu(\xi), & v_{01}(\xi) &= \sum_\nu c_{01}^\nu q_\nu(\xi).
\end{aligned} \tag{27}$$

Substitution of these expressions into Eqs. (26) gives a system of linear equations for the coefficients b^ν , c^ν which is straightforward to solve. For the out-of-phase dressed-state the spectrum of the elementary excitations is

$$\omega = \left\{ \pm \sqrt{\left(\nu + \frac{1}{2} + \frac{1}{2}\xi_m^2\right) \left(\nu + \frac{1}{2}\right)}, \pm \sqrt{\left(\nu + \frac{1}{2} + \frac{1}{2}\xi_m^2\right) \left(\nu + \frac{1}{2} + 2g\right)} \right\}. \quad (28)$$

Both branches of normal modes given by Eq. (28) are stable, as they are characterized by real values of ω . In contrast, the spectrum of the normal modes for the in-phase dressed-state is

$$\omega = \left\{ \pm \sqrt{\left(\nu + \frac{1}{2} + \frac{1}{2}\xi_m^2 - 2g\right) \left(\nu + \frac{1}{2} - 2g\right)}, \pm \sqrt{\left(\nu + \frac{1}{2} + \frac{1}{2}\xi_m^2\right) \left(\nu + \frac{1}{2}\right)} \right\}. \quad (29)$$

There are again two branches in the excitation spectrum, one of which,

$$\omega = \pm \sqrt{\left(\nu + \frac{1}{2} + \frac{1}{2}\xi_m^2 - 2g\right) \left(\nu + \frac{1}{2} - 2g\right)}$$

can become unstable, that is, ω can assume imaginary values. In particular, the region of instability is defined in terms of the index ν of the linear oscillator mode as

$$\begin{aligned} 2g - \frac{1}{2}\xi_m^2 < \nu + \frac{1}{2} < 2g & \quad \text{for} \quad g > \frac{1}{4}\xi_m^2; \\ \nu + \frac{1}{2} < 2g & \quad \text{for} \quad g < \frac{1}{4}\xi_m^2. \end{aligned} \quad (30)$$

A detailed analysis of the eigenmodes corresponding to the elementary excitations reveals that for the in-phase dressed state the unstable excitations have normal modes that are π out of phase, that is, $u_{10}(\xi) = -u_{01}(\xi)$ and $v_{10}(\xi) = -v_{01}(\xi)$, whereas the system is stable against symmetric perturbations, $u_{10}(\xi) = u_{01}(\xi)$ and $v_{10}(\xi) = v_{01}(\xi)$. This means that as the instability develops, the density profiles of the (1,0) and (0,1) components should display modulations which are π out of phase.

From this analysis we can also estimate the index ν_{max} for the mode of largest growth rate, that is, the most negative value of

$$f(\nu) \equiv \omega^2 = \left(\nu + \frac{1}{2} + \frac{1}{2}\xi_m^2 - 2g\right) \left(\nu + \frac{1}{2} - 2g\right).$$

The requirement $f'(\nu) = 0$ then leads to the condition

$$\nu_{max} + \frac{1}{2} = 2g - \frac{1}{4}\xi_m^2, \quad (31)$$

where the nearest integer value should be taken for ν_{max} . The corresponding growth rate is readily found to be $Im(\omega) = \eta|\theta_{10}(0)|^2 \approx \xi_m^2/4$.

D. Numerical simulation of instability

In this section we present sample numerical simulations of the development of the predicted instability for the in-phase dressed state BEC. The aim of these simulations is to validate the approximate stability analysis of the previous section, and to put its predictions in context using a concrete example.

We have solved the coupled Gross-Pitaevskii equations (20) using a standard beam propagation technique for the initial conditions

$$\phi_{10}(\xi, 0) = \sqrt{1 + \epsilon}\theta_{10}(\xi), \quad \phi_{01}(\xi, 0) = \sqrt{1 - \epsilon}\theta_{10}(\xi), \quad (32)$$

where $\theta_{10}(\xi) = \theta_{01}(\xi)$ is the in-phase ground state. In the initial condition (32) the parameter $\epsilon \ll 1$ is included to provide a slight deviation from the exact in-phase solution. This deviation from the exact ground state of the trapping potential can be viewed as a wave packet of the normal modes, which triggers any instability present in the system.

We numerically generated the in-phase ground state solution by evolving the Thomas-Fermi ground state (22), which represents a symmetric perturbation of the system and is hence stable, until the density profile reached a steady-state. This evolution of the initial Thomas-Fermi solution towards the actual ground state occurs since in our numerical scheme an absorber is placed at the spatial grid boundaries to avoid unphysical reflections of high spatial frequencies: The absorber removes the high spatial frequencies present in the Thomas-Fermi solution leaving behind the actual ground state solution for which the absorber has a negligible effect.

For the numerical simulations presented here we have set $\eta = 80$, and thus $\xi_m = 4.93 \gg 1$, so the approximations employed here should be valid. Figure 1 shows the density profile $|\phi_{10}(\xi, \tau)|^2$ for $\tau = 0$ (solid line) and $\tau = 2$ (dashed line), and $g = 0$ so there is no coupling. In this case the density profile remains close to the initial profile with no sign of any density modulations appearing, meaning that the system is stable against density oscillations. Figure 2 shows the evolution of the central densities $|\phi_{10}(0, \tau)|^2$ and $|\phi_{01}(0, \tau)|^2$ for $g = 7.29$. Initially, the densities show modulations resulting from the beating of the normal modes excited in the initial state, but this is followed by a region of exponential growth for one component and decay for the other. This is where the excitation of largest growth rate is expected to be dominant, and the predictions of the linear stability analysis can be tested. In particular, for the parameters used here we find $\nu_{max} = 8$ from Eq. (31). Figure 3 shows the density profiles $|\phi_{10}(\xi, \tau = 2)|^2$ (dotted line) and $|\phi_{01}(\xi, \tau = 2)|^2$ (dashed line), along with the initial profile (solid line) for comparison. Here we have plotted the densities for $\tau = 2$ in the region of exponential growth and density modulations signaling an instability are clearly seen. In particular, the density oscillations of the two components are π out of phase as predicted, and the oscillations correspond precisely to those expected for the most unstable mode with $\nu_{max} = 8$.

These results clearly show that the linear coupling and associated quantum superposition of the system wave function have a large effect: In contrast to the stable BEC shown in Fig. 1 for $g = 0$, the introduction of linear coupling via a single cavity photon is sufficient to render the N -atom condensate spatially unstable.

The density profiles shown in Fig. 3 are appropriate if we determine which cavity mode the photon occupies. For example, $|\phi_{10}(\xi, \tau)|^2$ is the density given that there is one photon in mode 1 and none in mode 2. In contrast, if no determination is made of which mode the photon occupies then the density profile is $Tr_f(\rho_{atom}) \equiv |\phi_{01}(\xi, \tau)|^2 + |\phi_{10}(\xi, \tau)|^2$, and this is shown in Fig. 4 where the density oscillations remain but with sufficiently reduced contrast. Here we see the possibility for a delayed choice experiment with a many-body system: imagine that the system is left to evolve and then released from the trap after which it falls under

gravity and its density profile is measured. If we measure which mode the photon occupies as the BEC is dropping we expect the large contrast density oscillations, whereas if we don't measure which mode the photon occupies we expect the low contrast density oscillations. In addition, the decision whether to measure the cavity photon or not can in principle be made after the BEC has left the cavity when the BEC and field no longer interact, thus providing a delayed choice experiment. Care should be taken, however, that the time at which the measurement is performed is within the linear growth range illustrated in Fig. 2.

IV. CONCLUSION AND OUTLOOK

In this paper, we have introduced the concept of dressed condensates, which permit to create a coupled, multicomponent macroscopic quantum system whose dynamics can be vastly different from that of a bare condensate. A number of immediate extensions of the ideas presented here can readily be envisioned. For example, one can easily imagine ways to create three-component systems, entangled condensates, etc. Such systems will allow one to extend many of the ideas related to measurement theory that have been developed in recent years in quantum optics to truly macroscopic quantum systems.

ACKNOWLEDGMENTS

This work is supported by the U.S. Office of Naval Research Contract No. 14-91-J1205, by the National Science Foundation Grant PHY95-07639, by the Joint Services Optics Program and by the US Army Research Office. The information contained in this paper does not necessarily reflect the position or policy of the U.S. Government, and no official endorsement should be inferred. P. M. gratefully acknowledges an Alexander-von-Humboldt Stiftung Award which enabled his stay at the Max-Planck Institut für Quantenoptik, during which part of this work was carried out. He also thanks Prof. H. Walther for his warm hospitality.

**APPENDIX A: FAR OFF-RESONANCE SINGLE-ATOM
EFFECTIVE HAMILTONIAN**

In Section I we introduced the Hamiltonian (2) which describes dynamics of a single-atom. This Hamiltonian conserves number of excitations in the system, and thus its state can be represented as a linear combination of the states with one excitation

$$|\psi(t)\rangle = \alpha_{00}(t)|e00\rangle + \alpha_{10}(t)|g10\rangle + \alpha_{01}(t)|g01\rangle. \quad (\text{A1})$$

Equations for the coefficients $\alpha_i(t)$ follow from the Schrödinger equation for the state $|\psi\rangle$ and read (here we omit kinetic energy and trapping potential terms)

$$\begin{aligned} i\dot{\alpha}_{00}(t) &= \delta\alpha_{00}(t) + \Omega_0(\alpha_{10}(t) + \alpha_{01}(t)) \\ i\dot{\alpha}_{10}(t) &= \Omega_0\alpha_{00}(t) \\ i\dot{\alpha}_{01}(t) &= \Omega_0\alpha_{00}(t) \end{aligned} \quad (\text{A2})$$

Assuming $\delta \gg 1$ the excited atomic state can be adiabatically eliminated

$$\alpha_{00}(t) = -\frac{\Omega_0}{\delta}(\alpha_{10}(t) + \alpha_{01}(t))$$

and the resulting equations for the coefficients $\alpha_{01}(t)$ and $\alpha_{10}(t)$ read

$$\begin{aligned} i\dot{\alpha}_{10}(t) &= -\frac{\Omega_0^2}{\delta}(\alpha_{10}(t) + \alpha_{01}(t)) \\ i\dot{\alpha}_{01}(t) &= -\frac{\Omega_0^2}{\delta}(\alpha_{10}(t) + \alpha_{01}(t)). \end{aligned} \quad (\text{A3})$$

At this point it is straightforward to see that these equations follow from the Schrödinger equation for the state

$$|\psi_{eff}(t)\rangle = \alpha_{10}(t)|10\rangle + \alpha_{01}(t)|01\rangle$$

if the effective Hamiltonian for the system is (3).

REFERENCES

- ¹ M.H. Anderson, J.R. Ensher, M.R. Matthews, C.E. Wieman, and E.A. Cornell, *Science* **269**, 198 (1995).
- ² K. B. Davis, M.-O. Mewes, M. R. Andrews, N. J. van Druten, D. S. Durfee, D. M. Kurn, and W. Ketterle, *Phys. Rev. Lett.* **75**(22), 3969 (1995).
- ³ E. M. Lifshitz and L. P. Pitaevskii. *Statistical Physics, Part 2*. Pergamon Press, New York, 1980.
- ⁴ M. Edwards and K. Burnett, *Phys. Rev. A* **51**, 1382 (1995).
- ⁵ P. A. Ruprecht, M. J. Holland, K. Burnett, and M. Edwards, *Phys. Rev. A* **51**, 4704 (1995).
- ⁶ G. Baym and C. J. Pethick, *Phys. Rev. Lett.* **76**, 6 (1996).
- ⁷ A. L. Fetter, *Phys. Rev. A* **53**, 4245 (1996).
- ⁸ S. Stringari, *Phys. Rev. Lett.* **77**, 2360 (1996).
- ⁹ K. G. Singh and D. S. Rokhsar, *Phys. Rev. Lett.* **77**, 1667 (1996).
- ¹⁰ M. Edwards, P. A. Ruprecht, K. Burnett, R. J. Dodd, and C. W. Clark, *Phys. Rev. Lett.* **77**, 1671 (1996).
- ¹¹ D. S. Jin, J. R. Ensher, M.R. Matthews, C. E. Wieman, and E. A. Cornell, *Phys. Rev. Lett.* **77**, 420 (1996).
- ¹² M.-O. Mewes, M. R. Andrews, N. J. van Druten, D. M. Kurn, D. S. Durfee, C. G. Townsend, and W. Ketterle, *Phys. Rev. Lett.* **77**, 988 (1996).
- ¹³ A. Griffin, *Phys. Rev. B* **53**, 9341 (1996).
- ¹⁴ Yu. Kagan, G. V. Shlyapnikov, and J. T. M. Walraven, *Phys. Rev. Lett.* **76**, 2670 (1996).
- ¹⁵ J. R. Ensher, D. S. Jin, M. R. Matthews, C. E. Wieman, and E. A. Cornell, *Phys. Rev.*

- Lett.* **77**, 4984 (1996).
- ¹⁶ M.-O. Mewes, M. R. Andrews, N. J. van Druten, D. M. Kurn, D. S. Durfee, and W. Ketterle, *Phys. Rev. Lett.* **77**, 416 (1996).
- ¹⁷ A. C. Newell, T. Passot, and J. Lega, *Annu. Rev. Fluid Mech.* **25**, 399 (1993).
- ¹⁸ S. Coleman. *Aspects of Symmetry*. Cambridge University Press, New York, 1983.
- ¹⁹ A. C. Newell and J. V. Moloney. *Nonlinear Optics*. Addison-Wesley, Redwood City, Calif., 1992.
- ²⁰ *Chaos, Solitons and Fractals*, Special issue: Nonlinear optics, structures, patterns, chaos **4** (1994).
- ²¹ G. P. Agrawal. *Nonlinear Fiber Optics*. Academic Press, New York, 1995.
- ²² J. C. Eilbeck, P. S. Lomdahl, and A. C. Scott, *Physica D* **16**, 318 (1985).
- ²³ C. J. McKinstrie and G. G. Luther, *Phys. Ser.* **30**, 31 (1990).
- ²⁴ E. V. Goldstein and P. Meystre, *Phys. Rev. A* **55**, 2935 (1997).
- ²⁵ C. J. Myatt, E. A. Burt, R. W. Ghrist, E. A. Cornell, and C. E. Wieman, *Phys. Rev. Lett.* **78**, 586 (1997).
- ²⁶ P. S. Julienne, F. H. Mies, E. Tiesinga, and C. J. Williams, *Phys. Rev. Lett.* **78**, 1880 (1997).
- ²⁷ P. O. Fedichev, Yu. Kagan, G. V. Shlyapnikov, and J. T. M. Walraven, *Phys. Rev. Lett.* **77**, 2913 (1996).
- ²⁸ C. Cohen-Tannoudji, J. Dupont-Roc, and G. Grynberg. *Atom-Photon Interaction. Basic Processes and Applications*. New York : Wiley, New York, 1992.
- ²⁹ S. Haroche. Cavity quantum electrodynamics. In J. Dalibard, J.-M. Raimond, and J. Zinn-Justin, editors, *Fundamental Systems in Quantum Optics*, page 546. North-

Holland, Amsterdam, 1992.

³⁰ P. Meystre and M. Sargent III. *Elements of Quantum Optics*. Springer-Verlag, Heidelberg, 1991.

³¹ J. W. Negele, *Rev. Mod. Phys.* **54**, 913 (1982).

³² S. Trillo, S. Wabnitz, E. M. Wright, and G. I. Stegeman, *Opt. Lett.* **13**, 672 (1988).

³³ N. N. Bogoliubov, *J. Phys. USSR* **11**, 23 (1947).

FIGURES

FIG. 1. Evolution of the density profile $|\phi_{01}(\xi, \tau)|^2$ at $\tau = 2$ (dashed line) from the initial ground state solution (solid line) without linear coupling $g = 0$. In this figure and all others we set $\eta = 80$.

FIG. 2. Time dependence of the densities $|\phi_{01}(\xi, \tau)|^2$ (dashed line) and $|\phi_{10}(\xi, \tau)|^2$ (solid line) at the center of the trapping potential showing the region of exponential growth for the case with linear coupling $g = 7.29$.

FIG. 3. Oscillatory pattern developed on top of the ground state profile in the exponential growth region $\tau = 2$: Ground state solution (solid line), $|\phi_{10}(\xi, \tau)|^2$ (dotted line), and $|\phi_{01}(\xi, \tau)|^2$ (dashed line).

FIG. 4. Total density $|\phi_{10}(\xi, \tau)|^2 + |\phi_{01}(\xi, \tau)|^2$ at $\tau = 2$ in the region of exponential growth for the case that no determination is made of which mode the photon occupies.

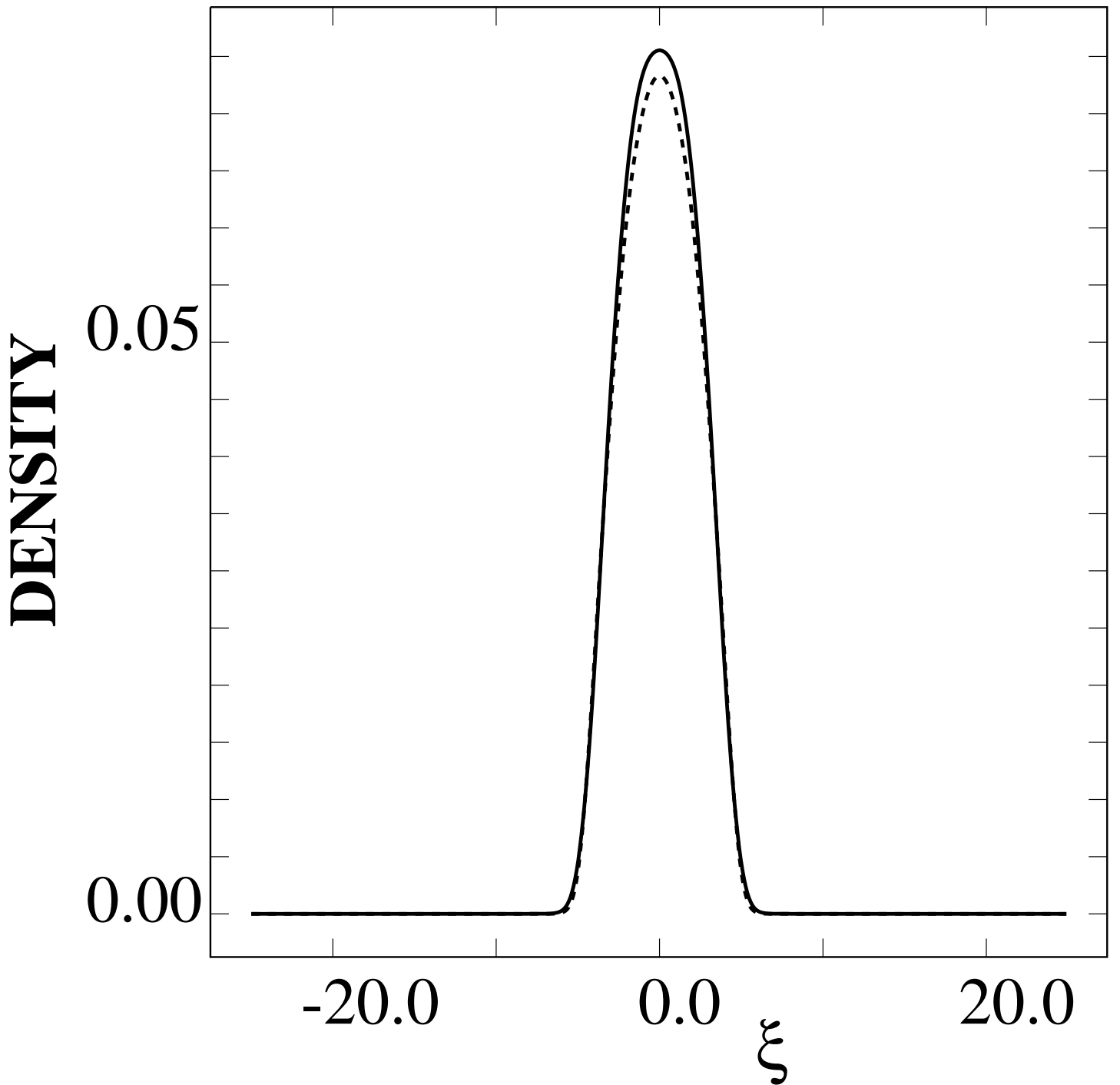


Fig. 1

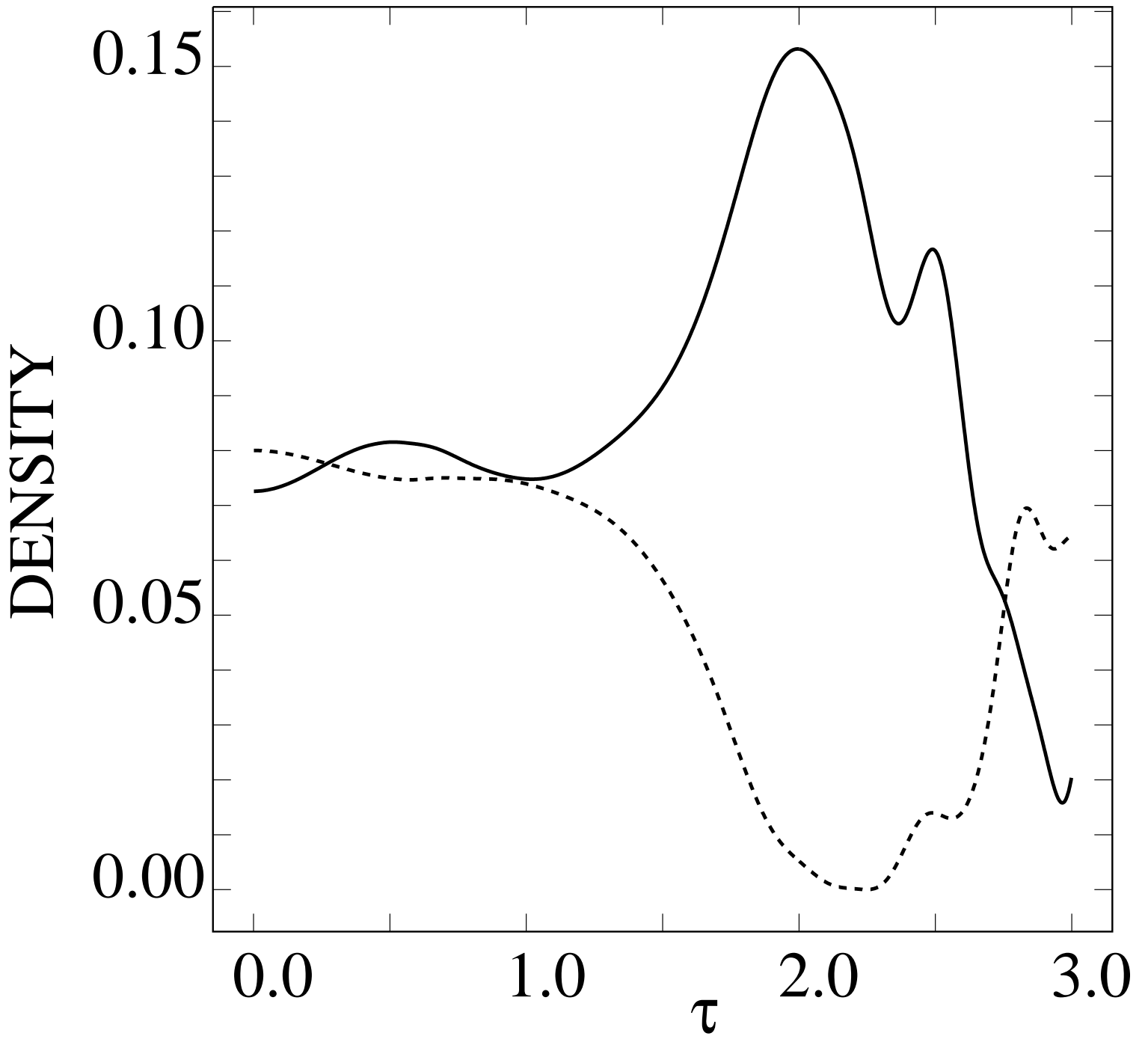


Fig. 2

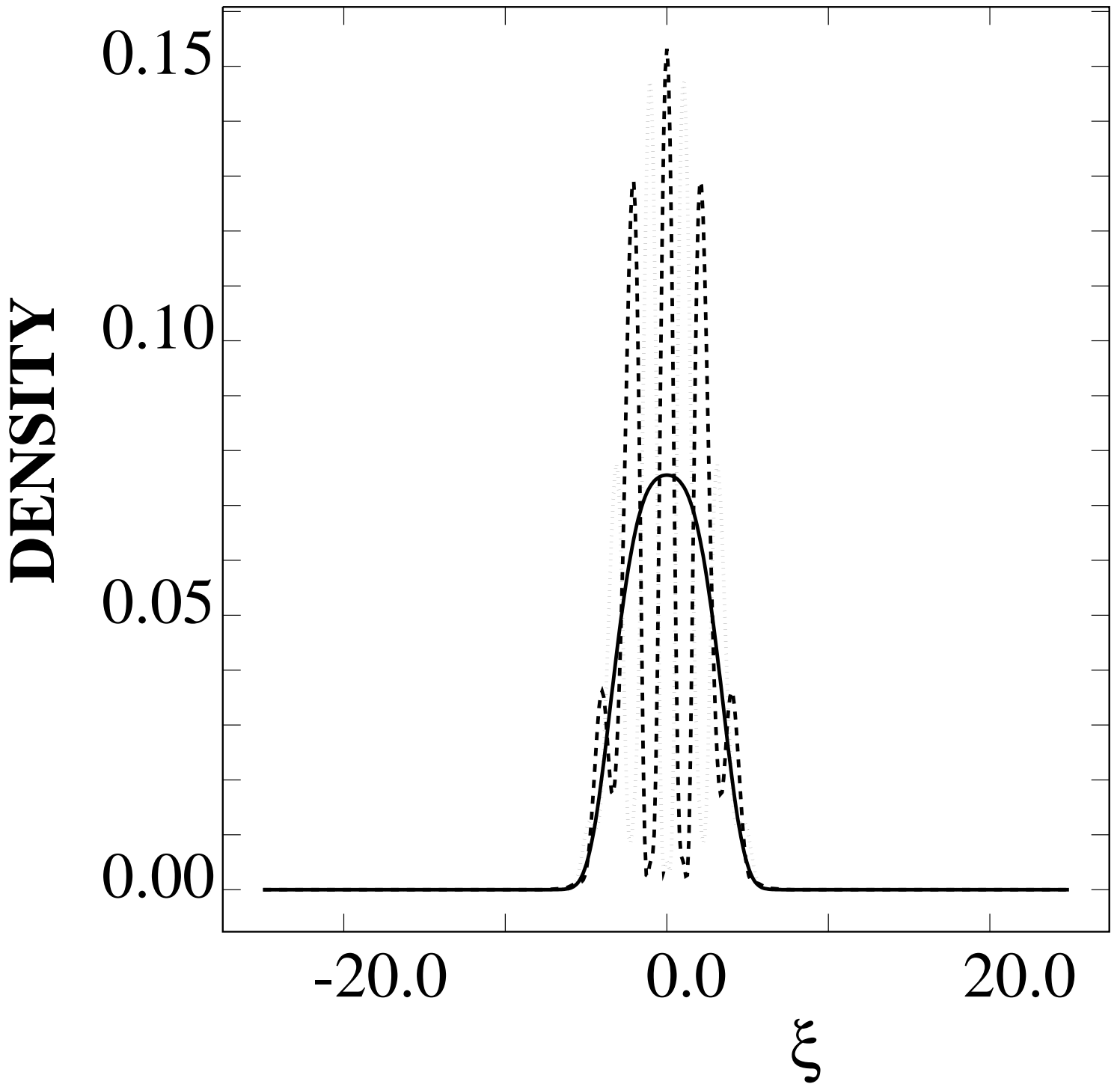


Fig. 3

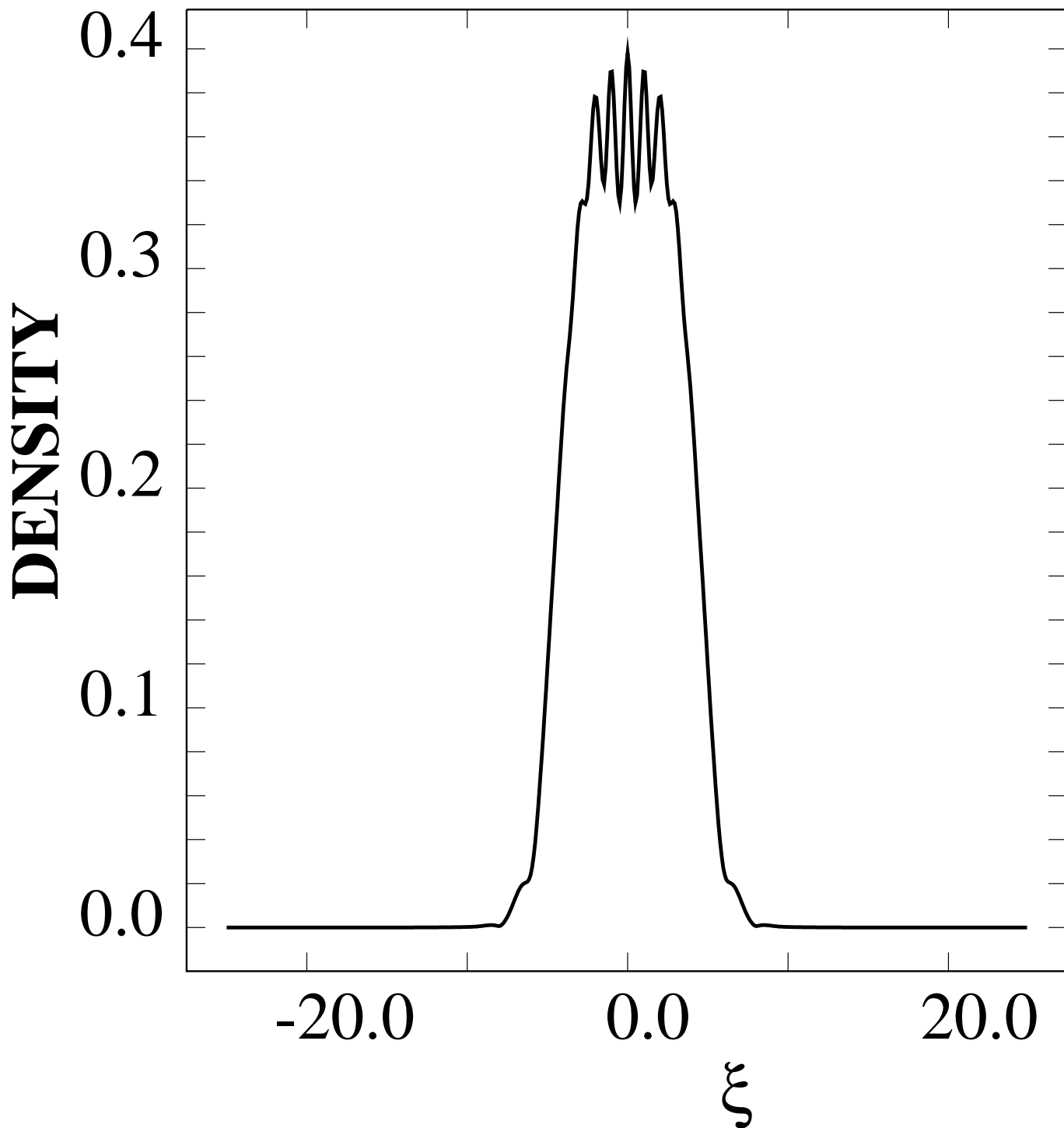


Fig. 4